Superluminal Caustics of Close, Rapidly-Rotating Binary Microlenses

Zheng Zheng and Andrew Gould The Ohio State University, Columbus, OH 43210, USA E-mail: zhengz, gould@astronomy.ohio-state.edu

ABSTRACT

The two outer triangular caustics (regions of infinite magnification) of a close binary microlens move much faster than the components of the binary themselves, and can even exceed the speed of light. When $\epsilon \gtrsim 1$, where ϵc is the caustic speed, the usual formalism for calculating the lens magnification breaks down. We develop a new formalism that makes use of the gravitational analog of the Liénard-Wiechert potential. We find that as the binary speeds up, the caustics undergo several related changes: First, their position in space drifts. Second, they rotate about their own axes so that they no longer have a cusp facing the binary center of mass. Third, they grow larger and dramatically so for $\epsilon \gg 1$. Fourth, they grow weaker roughly in proportion to their increasing size. Superluminal caustic-crossing events are probably not uncommon, but they are difficult to observe.

Subject headings: gravitational lensing – binary systems

1. Introduction

Microlensing is gravitational lensing where the separations between the images are too small to be resolved. The directly detectable consequence of microlensing is that the brightness of the source varies in a way determined by the lens properties and the projected lens-source trajectory. Paczyński (1986) pointed out that microlensing would be a useful tool to detect massive compact halo objects. Microlensing surveys have since been carried out towards the Galactic bulge, the Magellanic Clouds, and M31. About 500 microlensing events have been detected to date (see Mao 2000 for a review).

Gravitational lensing by two point masses was carefully studied by Schneider & Weiss (1986). The most striking feature of such binary lensing is its caustics - one or several closed curves in the source (objects to be imaged) plane where a point source is infinitely magnified by the lens. As a reflection of the caustic structure of the magnification, the light curves of such binary lensing events may have multiple peaks. Microlensing surveys have detected about 30 such events (e.g., Udalski et al. 1994; Alcock et al. 2000). Star-planetary systems are an extreme form of binary. Mao & Paczyński (1991) first suggested that extrasolar planetary systems could be discovered by microlensing surveys.

Dominik (2000) conducted the first systematic investigation of the effect of binary rotation on microlensing light curves. Although all physical binaries rotate, static models suffice to reproduce the light curves of the great majority of observed microlensing events, even those with superb data such as MACHO 97-BLG-28 (Albrow et al. 1999a) and MACHO 98-SMC-1 (Afonso et al. 2000). The only event observed to date for which a rotating model is required is MACHO 97-BLG-41 (Albrow et al. 2000), and static models are excluded for this event only because the source traverses two disjoint caustics, a rare (so far, unique) occurrence. Bennett et al. (1999) had earlier proposed that the odd light curve of MACHO 97-BLG-41 could be explained by a triple-lens system consisting of a binary plus a jovian-mass planet.

In the treatments of binary rotation given to date (Dominik 1998; Albrow et al. 2000), the light curve is actually calculated by considering a series of *static* binaries, each with the configuration of the binary being modeled at the *instant* when the light ray from the source passes the plane of the center of mass of the lens. That is, the deflection of light by the binary, α , is taken to be the vector sum of the deflections produced by the two components of the binary, $\alpha = \alpha_1 + \alpha_2$, according to the Einstein (1936) formula,

$$\boldsymbol{\alpha}_i = -\frac{4GM_i}{b_i^2 c^2} \mathbf{b}_i. \tag{1}$$

Here M_i is the mass, and \mathbf{b}_i is the impact parameter of the *i*th component of the binary.

This approach is strictly valid only in the limit

$$\epsilon \ll 1, \qquad \epsilon \equiv \frac{\omega b}{c},$$
(2)

where $2\pi/\omega$ is the period of the binary. For MACHO 97-BLG-41, the only microlensing event for which rotation has been measured (Albrow et al. 2000), $\epsilon \sim 10^{-4}$, so this approach is certainly valid. However, in principle ϵ can be close to unity or can even greatly exceed unity. In this case, it is necessary to take account of the binary motion during the time that the source light is passing close ($\leq b$) to the lens plane. The Einstein formula (1), which was calculated for a static lens, is then no longer valid.

Here we study the rotation effects on the caustic structure of close, rapidly-rotating binary lenses. We present our main idea and method in \S 2 and discuss the rotation effects in \S 3. In \S 4, we summarize our results and discuss some possible applications.

2. Main Idea and Method

As mentioned in § 1, the binary phase varies during the time that the photons are traveling from the source to the observer. This modifies the calculation of the instantaneous magnification map, especially for $\epsilon \gtrsim 1$. The retarded gravitational potential then begins to differ significantly from the naive Newtonian potential, which would normally be adequate in the weak-field limit and which is used to derive equation (1).

2.1. Retarded Gravitational Potential

As an approximate result of Einstein's field equations, the deflection of a light ray passing through a static gravitational field can be expressed as an integral of the gradient of the Newtonian gravitational potential performed along the trajectory of the light (Bourassa et al. 1973):

$$\boldsymbol{\alpha} = -\frac{2}{c} \int_{-\infty}^{+\infty} \nabla \phi \, \mathrm{d}t,\tag{3}$$

which yields equation(1). However, for the non-static case, the configuration of the gravitational field will propagate at light speed, and we must instead use the retarded potential.

In analogy to the results of classical electrodynamics (e.g. Jackson 1975), the gravitational potential at field point \mathbf{r} and time t is contributed by every mass point \mathbf{r}' at an earlier time $t' = t - |\mathbf{r} - \mathbf{r}'|/c$,

$$\phi(\mathbf{r},t) = -\int \frac{G\rho(\mathbf{r}',t')}{|\mathbf{r} - \mathbf{r}'|} d^3 \mathbf{r}', \tag{4}$$

where ρ is the (time-dependent) mass distribution.

For a point mass M, the retarded potential (4) can be written, similarly to the Liénard-Wiechert potential,

$$\phi(\mathbf{r},t) = -\frac{GM}{(1 - \mathbf{n}' \cdot \boldsymbol{\beta}')|\mathbf{r} - \mathbf{r}'|},\tag{5}$$

where $\mathbf{n}' = (\mathbf{r} - \mathbf{r}')/|\mathbf{r} - \mathbf{r}'|$, $\boldsymbol{\beta}'$ is the velocity of the point mass divided by c, and the prime denotes the value at time t',

$$t = t' + \frac{|\mathbf{r} - \mathbf{r}'(t')|}{c}.$$
 (6)

The Newtonian gravitational field, $\mathbf{g} = -\nabla \phi$, is then

$$\mathbf{g}(\mathbf{r},t) = \left[\nabla \frac{GM}{(1-\mathbf{n} \cdot \boldsymbol{\beta})|\mathbf{r} - \mathbf{r}'|} \right]_{t'} = \left[-\frac{GM}{(1-\mathbf{n} \cdot \boldsymbol{\beta})^2 |\mathbf{r} - \mathbf{r}'|^2} (\mathbf{n} + \boldsymbol{\beta}) \right]_{t'}.$$
 (7)

For those rays that pass across the lens at a distance much greater than the Schwarzschild radius $2GM/c^2$, the total deflection angle caused by several lens objects is a superposition of the individual deflections (Bourassa et al. 1973). From equations (3) and (7), we have,

$$\boldsymbol{\alpha} = -\sum_{i} \frac{2GM_{i}}{c} \int_{-\infty}^{+\infty} \left[\frac{\mathbf{n}_{i} + \boldsymbol{\beta}_{i}}{(1 - \mathbf{n}_{i} \cdot \boldsymbol{\beta}_{i})^{2} |\mathbf{r} - \mathbf{r}_{i}|^{2}} \right]_{t'} dt.$$
 (8)

It is convenient to take the time when the photon crosses the lens plane as t = 0. Then at a distance |ct| to the lens plane, the photon will feel the potential caused by the point mass M_i at time t'. We have

$$|\mathbf{r} - \mathbf{r}_i(t')| = \sqrt{b_i^2(t') + (ct)^2},$$
 (9)

where $b_i(t')$ is the distance from the point mass M_i to the impact point at time t'. Substitution of equation (9) into equation (6) yields

$$t = \frac{1}{2}t' - \frac{b_i^2(t')}{2c^2t'}. (10)$$

This relation between t and t' reflects the retarded effect. For a finite $b_i(t')$, and under the condition t > t', we find that when $t \to -\infty$, $t' \to -\infty$ and when $t \to +\infty$, $t' \to 0^-$. That is $t' \simeq 2t$ when $t \ll 0$ and $t' \simeq 0$ when $t \gg 0$. For a circular orbit, this means that as a photon moves towards the rotating system, it will "find" that the angular velocity of the system is nearly doubled, and as it moves away from the system, it will feel an almost static field. Equation (10) makes it possible to replace the integration variable in equation (8) with t' (from $-\infty$ to 0).

2.2. Lens Equation

The lens equation, i.e. the light-ray deflection equation, tells one how the light-ray deflection maps points in the source plane into points in the image plane (lens plane). If a photon comes from point η in the source plane and hits point ζ in the lens plane, we have (Schneider & Weiss 1986),

$$\boldsymbol{\eta} = \frac{D_s}{D_l} \boldsymbol{\zeta} - D_{ls} \boldsymbol{\alpha}(\boldsymbol{\zeta}), \tag{11}$$

where D_s and D_l are the distances from the observer to the source plane and to the lens plane, respectively, and $D_{ls} = D_s - D_l$ is the distance between the source and the lens.

In this paper, we consider a simple case: the lens is composed of two stars with equal masses $M_1 = M_2$, rotating about each other in a circular face-on orbit. We define the distance between two stars to be 2a and the angular velocity around the center of mass to be ω (see Fig. 1). We define the radius of the Einstein ring generated by the total mass $M_1 + M_2$ to be (e.g. Schneider & Weiss 1986)

$$r_{\rm E} = \sqrt{\frac{4G(M_1 + M_2)}{c^2} \frac{D_l D_{ls}}{D_s}},$$
 (12)

and then normalize the coordinates of points at the lens plane and those at the source plane using this radius and the radius projected onto the source plane, respectively:

$$X = \frac{a}{r_{\rm E}},\tag{13}$$

$$\mathbf{r} = \frac{\zeta}{r_{\rm E}},\tag{14}$$

$$\mathbf{x} = \boldsymbol{\eta} \left[r_{\rm E} \frac{D_s}{D_l} \right]^{-1}. \tag{15}$$

The consequent lens equation is given in Appendix A.

The focus of the present study is the case $X \ll 1$, for which there are two small triangular caustics lying at projected distances $\sim r_{\rm E}/(2X)$ from the binary center of mass (Schneider & Weiss 1986). As the binary rotates at angular speed ω , the caustics rotate with it. Hence the transverse speed of the caustics is $v/(2X^2)$, where $v=\omega a$ is the speed of the binary components. For very small X, the caustics can move much faster than the speed of light ("superluminal motion") even when the binary itself is well within the non-relativistic regime.

Since we have fixed the mass ratio, $M_2/M_1=1$, and adopted a face-on, circular orbit, there are only three free parameters of the lens system, X, ω , and a. However, from the standpoint of studying the caustic structure that appears in diagrams from which all physical dimensions have been scaled out, it is only necessary to consider *dimensionless* parameters. There are two independent such parameters. One is X. There are two obvious possible choices for the other,

$$\beta = \frac{\omega a}{c}, \qquad \epsilon = \frac{\omega r_{\rm E}}{2cX} = \frac{\beta}{2X^2}.$$
 (16)

The first is the speed of the lenses as a fraction of the speed of light, and the second is approximately the speed of the caustics as a fraction of the speed of light. As we show in the next section, ϵ is a more useful parameter than β because the caustics are more directly affected by their own speed rather than that of the lenses.

To make a two-dimensional magnification map of the lens system (around the caustics), we use the inverse ray-shooting technique (e.g., Schneider & Weiss 1986; Wambsganss 1997). Uniformly distributed light rays in the lens plane are evolved back to the source plane according to the lens equation. The magnification of each point in the source plane is then proportional to the density of rays at this point. We study the cases of X = 0.1, X = 0.05 with various values of ϵ .

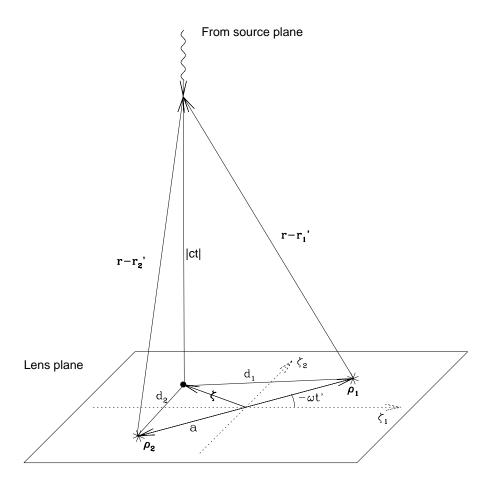


Fig. 1.— Geometry of the rotating binary lens with equal masses and face-on circular orbit. At time t, the photon feels a potential generated by the two stars at an earlier time t'.

3. Effects of the Rotation

Figure 2 displays some examples of the outer caustics generated by adopting different parameters. Compared with the static case, these caustics show some new features.

3.1. "Orbit Position" of the caustic

In the static case, the outer caustics of an equal-mass binary are located along the perpendicular bisector of the binary. If the binary lens rotates around the center while the photon is traveling, it is not hard to imagine that the consequent caustics will drift with respect to the bisector of the binary lens at phase t = 0. It turns out that the direction of this drift is opposite to the rotation. Physically, the reason for this "opposite" drifting is that at all times t, the phase of the binary corresponds to an earlier time t' < 0. See equation (10) and the analysis following it. In Figure 3, we show the angular position of the caustic relative to the static case as a function of β . For $\beta \lesssim 0.1$, we find a fitted formula for the "orbit" angle θ_{orbit} (in radians):

$$\theta_{orbit} = \frac{4}{7}\beta = \frac{8}{7}X^2\epsilon. \tag{17}$$

We find that the fitted coefficient in equation (17) is very close to the ratio of two small integers (4/7), but we do not know whether this result is exact.

3.2. "Spin" - Pointing of the caustic

Apart from the outer caustics' orbit motion as a whole, these "concave triangles" have their own rotation. We use the direction of a vertex (the one pointing to the center of mass in the static case) as a tracer for the caustic's "spin". Unlike the Moon which always shows the same hemisphere to the Earth, these triangles spin much faster than their orbital rotation. For the non-static case, they will no longer point to the center of mass. See Figure 4. The fitted formula for the spin angle θ_{spin} (in degrees) for $\epsilon < 2$ is

$$\log \theta_{spin} = 31.32 \log \epsilon + 0.02154. \tag{18}$$

3.3. "Expansion" - Enlargement of the caustic

For static case, it is known that the closer the binary is, the farther the triangular caustics are away from the center of mass and the smaller they become. The outer caustics shrink almost to a point in the case of very small X. However, after taking the rotation effect into account, we find that the tiny caustics are strikingly magnified. Meanwhile, unlike the static case, the shape of the caustics gradually loses its symmetry. We choose the area inside the caustic as a measure of the expansion effect. Since in the static case, the linear size of the outer caustic scales approximately as X^3 , we normalize the area in our case by X^6 . The expansion effect is illustrated in Figure 5.

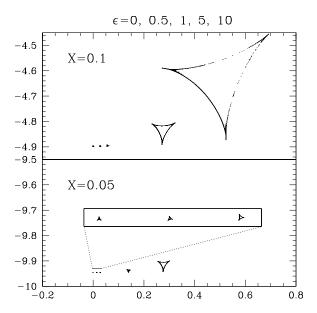


Fig. 2.— The outer caustics of a rapidly rotating binary lens. The upper and lower panels show the X=0.1 and X=0.05 cases, respectively. In each panel, caustics are shown $\epsilon=0,\,0.5,\,1,\,5,\,10$, from left to right, respectively. In the lower panel, the three smallest caustics are also shown expanded by a factor 20.

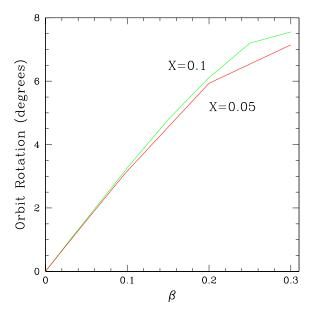


Fig. 3.— The orbit rotation angles of the outer caustics as a function of β .

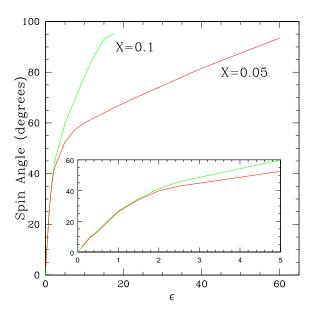


Fig. 4.— The spin angle of the outer caustics as a function of ϵ . The inset details the behavior for $\epsilon < 5$.

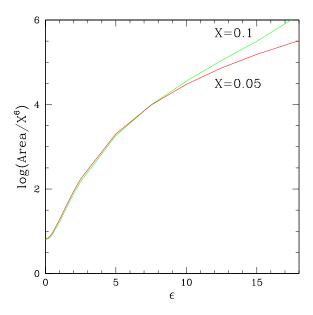


Fig. 5.— The expansion effect of the outer caustic. The area inside the caustic is normalized by X^6 .

3.4. Magnification Properties

The rapidly rotating binary lens makes the outer caustics move with a speed comparable to light speed which in turn brings some new phenomena to the magnification properties of the caustics.

First, the expansion of the outer caustic dilutes the magnification. In the static case, the magnification factor near a caustic curve can be described as $A(u) = A_0 + (\Delta u_{\perp}/u_r)^{-1/2}$, where Δu_{\perp} is the perpendicular distance to the caustic and A_0 and u_r are constants (Schneider & Weiss 1986; Schneider & Weiss 1987; Albrow et al. 1999b). Hence u_r describes the strength of the caustic. We investigate the variation of u_r as a function of ϵ and find that rapid rotation weakens the strength of the caustics. The relative strength of the three caustic lines (of the triangular caustic) also changes (see Fig. 6 for the case X = 0.1): one caustic line (left border, see Fig. 2) becomes the strongest one at large ϵ (large area). With a dimension of linear size, u_r is expected to scale as X^3 . However, our calculation shows that there is a slight deviation from this scale law: the change of u_r for X = 0.05 is a little steeper than that for X = 0.1. Taking account of our resolution, we are not sure whether this marginal effect is real or not.

Secondly, the velocity of the source with respect to the outer caustic is overwhelmingly determined by the caustic's high speed. The relative source-caustic trajectory is then a small piece of arc centered at the binary center of mass. The rapid rotation implies that the timescale for crossing the caustic will be very short. We choose the square root of the area S inside the caustic as the size of the caustic and the crossing time is then

$$t_c = \frac{\sqrt{S}}{\epsilon} \frac{r_{\rm E}}{c},\tag{19}$$

where $r_{\rm E}$ is the Einstein ring defined in equation (12). Since the area scales very nearly as X^6 (see Fig 5), this time scale can be normalized by X^3 . As shown in Figure 7, t_c has a minimum near $\epsilon \sim 1$. At smaller ϵ , becomes larger mainly due to the "low" speed of the caustic and at larger ϵ , mainly due to the expansion of the area.

4. Discussions

In this paper, we point out that a modification is necessary to get the instantaneous magnification map for close, rapidly-rotating binary lenses, in which case the outer caustics have a very high speed which can even be superluminal. Taking the retarded gravitational potential into consideration, we investigate the outer caustic behavior for such a lens with equal masses and face-on circular orbit. Compared with the static case, the caustic is displaced in orbit position and is rotated about its own axis. The most remarkable result is the enlargement of the caustic by the rapid motion of the lens. This increase in size induces a corresponding drop in the strength of the caustic.

Instead of starting from Einstein's field equation, we use a retarded potential at the first step. Although strictly speaking this method has its limitations, it is a reasonable approach for our purpose since our analysis focuses on the high speed of the outer caustics while the binary itself is not in the extreme relativistic regime.

What would be required to observe superluminal caustics? Combining the definitions of ϵ and $r_{\rm E}$ with Kepler's Third Law yields,

$$\epsilon = \frac{(2GM)^{3/2}D}{c^3 a^{5/2}} = 0.37 \left(\frac{M}{M_{\odot}}\right)^{3/2} \left(\frac{a}{0.1 \,\text{AU}}\right)^{-5/2} \frac{D}{2 \,\text{kpc}},\tag{20}$$

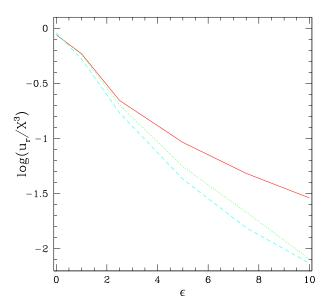


Fig. 6.— The strength u_r of the three caustic lines of the outer triangular caustic as a function of ϵ (for the case X=0.1, normalized by X^3). See text for the definition of u_r . The counterparts of the left, bottom and right caustic lines in the static case (see Fig. 2) are represented by the solid line, dashed line and dotted line, respectively.

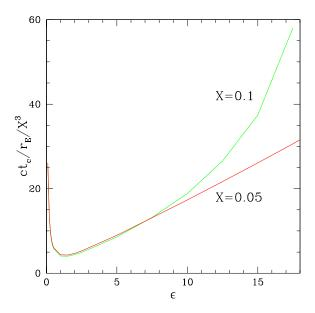


Fig. 7.— Time scale to cross the outer caustics in units of $r_{\rm E}/c$, normalized by X^3 , as a function of ϵ .

where $D = D_l D_{ls}/D_s$, M is the mass of one binary component, and where we have normalized to the case of a pair of solar-mass stars seen half way to the Galactic center. Equation (20) can be rewritten in terms of X,

$$X = 2^{-9/10} \epsilon^{-2/5} \left(\frac{GM}{Dc^2}\right)^{1/10}.$$
 (21)

Hence, to obtain $\epsilon \sim 1$ would require $X \sim 0.012$, a factor 4 smaller than even the lesser of the two values that we examined in this paper. Note that this result is extremely insensitive to either M or D.

From Figure 5, the combined cross section (linear size) of the two caustics at $\epsilon \sim 1$ is $S^{1/2} \sim 8X^3 r_{\rm E}$, that is, a factor $4X^3$ smaller than for the lens itself. For X=0.012, this factor is 10^{-5} , so that at first sight it appears completely hopeless that superluminal caustics would ever be observed. However, the event rate is the product of the cross section with the transverse speed, and the caustic moves $\sim 10^3$ times faster than transverse speed of the binary center of mass. In fact, since the caustic is likely to be smaller than the source, the event rate is given by the source size times the transverse speed of the caustic. Thus, the ratio of superluminal-caustic events to normal events generated by the same binary is

$$\frac{\Gamma_{\rm super}}{\Gamma_{\rm normal}} \sim \frac{2R_* D_l/D_s}{r_{\rm E}} \frac{\epsilon c}{v_{\perp}} \sim 1.2 \frac{R_*/R_{\odot}}{r_{\rm E}/6\,{\rm AU}} \frac{\epsilon}{v_{\perp}/200\,{\rm km\,s^{-1}}},\tag{22}$$

where R_* is the radius of the source, and v_{\perp} is the transverse speed of the binary center of mass. That is, they are about equally likely. Note that only a small minority (roughly a fraction X) of the superluminal events occur in association with a normal event (where the source passes within the Einstein ring). The rest are isolated "spike events". The real problem with observing superluminial events is not that they are uncommon, but that they are weak. For $\epsilon \lesssim 1$ the caustic covers (and hence magnifies) only a small fraction of the source star. For example, for $X=0.012, M=M_{\odot}, D_l=D_{ls}=4\,\mathrm{kpc}$, and $R=R_{\odot}$, the caustic covers only 0.01% of the source. Of course, for higher ϵ , the caustic area grows, but as we discuss in § 3.4, the strength of the caustic declines. Hence, at least for the present, superluminal caustics appear to be of mainly theoretical interest.

We thank Scott Gaudi for valuable discussions. This work was supported in part by grant AST 97-27520 from the NSF.

APPENDIX A

The lens equation can be written in terms of the normalized coordinates of points at the lens plane $\mathbf{r} = (r_1, r_2)$ and those at the source plane $\mathbf{x} = (x_1, x_2)$. It is convenient for calculation if we replace the integration variable t in equation (8) with t' using equation (10). Note that $-\infty < t' < 0$. According to the geometric relations in Figure 1, with the definition $\tau = ct'/a$, we then have the lens equation in component form:

$$x_i = r_i + \frac{1}{4} \int_{-\infty}^{0} [F_{1i}(\tau) + F_{2i}(\tau)] X d\tau,$$
 (A1)

where i = 1, 2 and

$$F_{i1} = \frac{4X\tau[r_1 + (-1)^i X \cos \beta \tau]}{(1 - p_i)[(X\tau)^2 + d_i^2(\tau)]^2} - \frac{2(-1)^i \beta \sin \beta \tau}{(1 - p_i)[(X\tau)^2 + d_i^2(\tau)]},\tag{A2}$$

$$F_{i2} = \frac{4X\tau[r_2 - (-1)^i X \sin \beta \tau]}{(1 - p_i)[(X\tau)^2 + d_i^2(\tau)]^2} - \frac{2(-1)^i \beta \cos \beta \tau}{(1 - p_i)[(X\tau)^2 + d_i^2(\tau)]},\tag{A3}$$

$$d_i^2(\tau) = [r_1 + (-1)^i X \cos \beta \tau]^2 + [r_2 - (-1)^i X \sin \beta \tau]^2, \tag{A4}$$

$$p_i = (-1)^{i-1} \frac{2X\beta\tau}{(X\tau)^2 + d_i^2(\tau)} (r_1 \sin\beta\tau + r_2 \cos\beta\tau). \tag{A5}$$

REFERENCES

Afonso, C., et al. 2000, ApJ, 532, 000 (astro-ph/9907247)

Albrow, M.D., et al. 1999a, ApJ, 522, 1011

Albrow, M.D., et al. 1999b, ApJ, 522, 1022

Albrow, M.D., et al. 2000, ApJ, 534, 000 (astro-ph/9910307)

Alcock, C. et al. 2000, ApJ, submitted (astro-ph/9907369)

Bennett, D.P., et al. 1999, Nature, 402, 57

Bourassa, R.R., Kantowski, R., & Norton, T.D. 1973, ApJ, 185, 747

Dominik, M. 1998, A&A, 329, 361

Einstein, A. 1936, Science, 84, 506

Jackson, J.D. 1975, Classical Electrodynamics, p. 654 (New York: Wiley)

Mao, S. 2000, in Gravitational Lensing: Recent Progress and Future Goals, eds. T.G. Brainerd and C.S. Kochanek, in press (astro-ph/9909302)

Mao, S., & Paczyński, B. 1991, ApJ, 374, L37

Paczyński, B. 1986, ApJ, 304, 1

Schneider, P., & Weiss, A. 1986, A&A, 164, 237

Schneider, P., & Weiss, A. 1987, A&A, 171, 49

Udalski, A. et al. 1994, ApJ, 436, L103

Wambsganss, J. 1997, MNRAS, 284, 172